Indo-Pacific climate interactions and control on rainfall

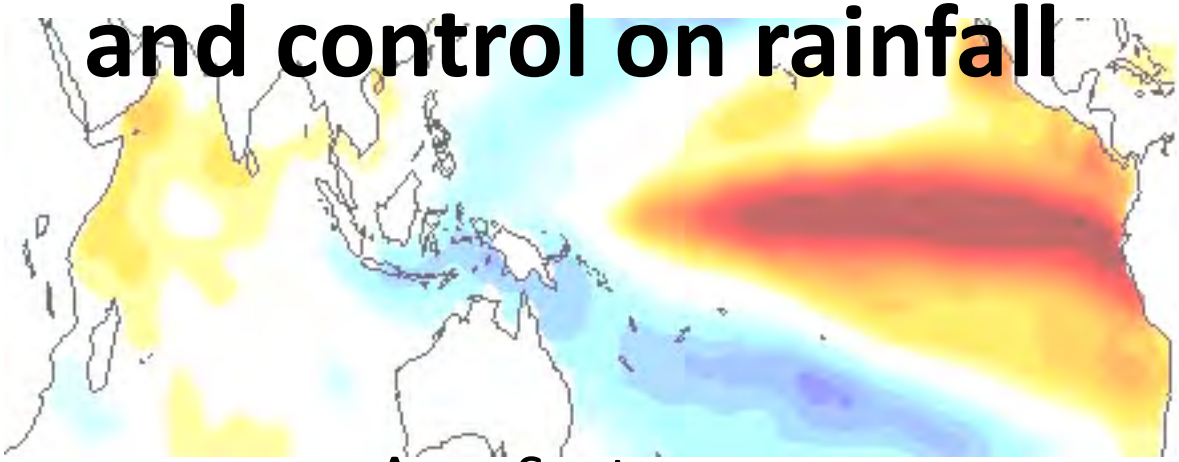

Agus Santoso
a.santoso@unsw.edu.au
Climate Change Research Centre (CCRC)
University of New South Wales, Sydney, Australia

In collaboration with:
Matthew England (CCRC), Wenju Cai (CSIRO CMAR)

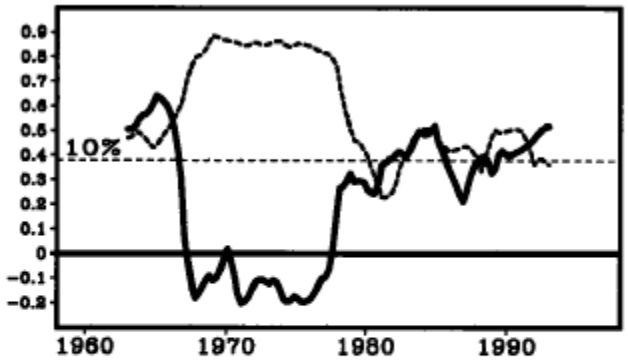

Figure 1. The 41-month sliding correlation coefficients between ISMR and IODMI (solid), and those between monthly ISMR and NINO3 SST (dashed; to be multiplied by −1) during 1958-1997. The significant correlation value at 90% confidence level is 0.38 (verified by 1,000 randomized time series, using the Monte-Carlo simulations)

Ashok et al. (2001, GRL 28)

Weaker (stronger) ENSO (IOD) influence on Indian summer monsoon rainfall since late 70's, accompanied by strengthening ENSO-IOD coherence.

So, ENSO and IOD co-occurrences influence rainfall.

DMI vs Nino3

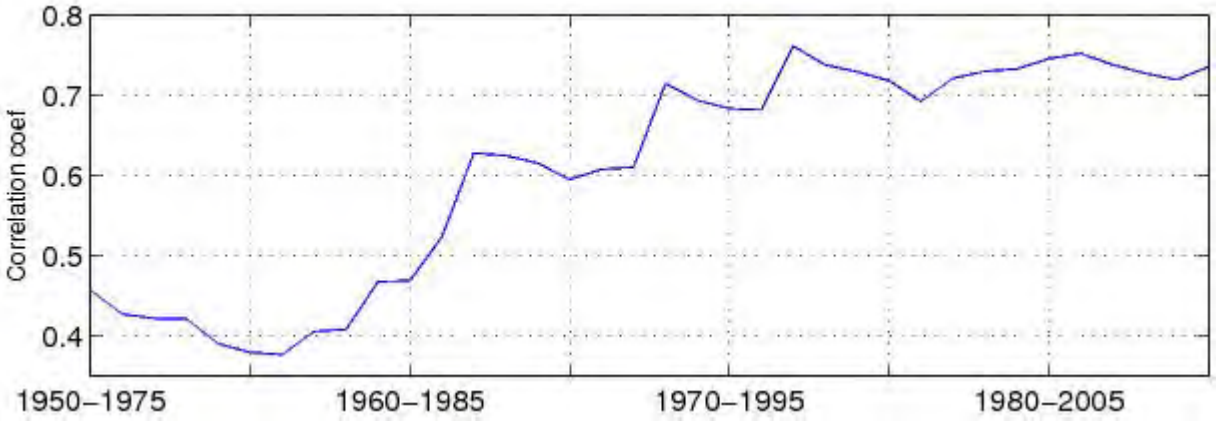

25-yr sliding window

A shift in ENSO dynamics

(e.g., Neelin et al. 1998; Fedorov and Philander 2001)

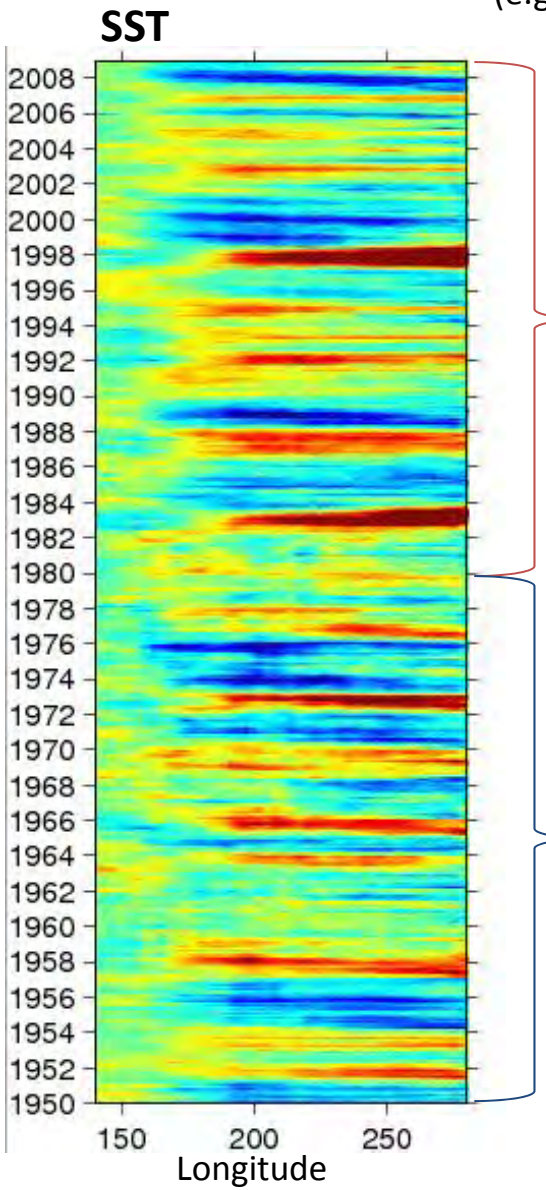

Thermocline mode

Eastward propagating SST anomalies - involving subsurface variability (i.e., mean upwelling acting on vertical gradient of anomalous temperature)

Local mode

Westward propagating SST anomalies - local SST-wind feedback (zonal advective + Ekman pumping)

Stronger anomalies

Note the asymmetry in zonal propagation of the warm and cold T-mode anomalies

Is the Indian Ocean part of ENSO dynamics?

Developing El Nino is often accompanied by a positive IOD. However, pre 1976 El Nino events often co-occur with a basin-wide warming (Annamalai et al. 2005):

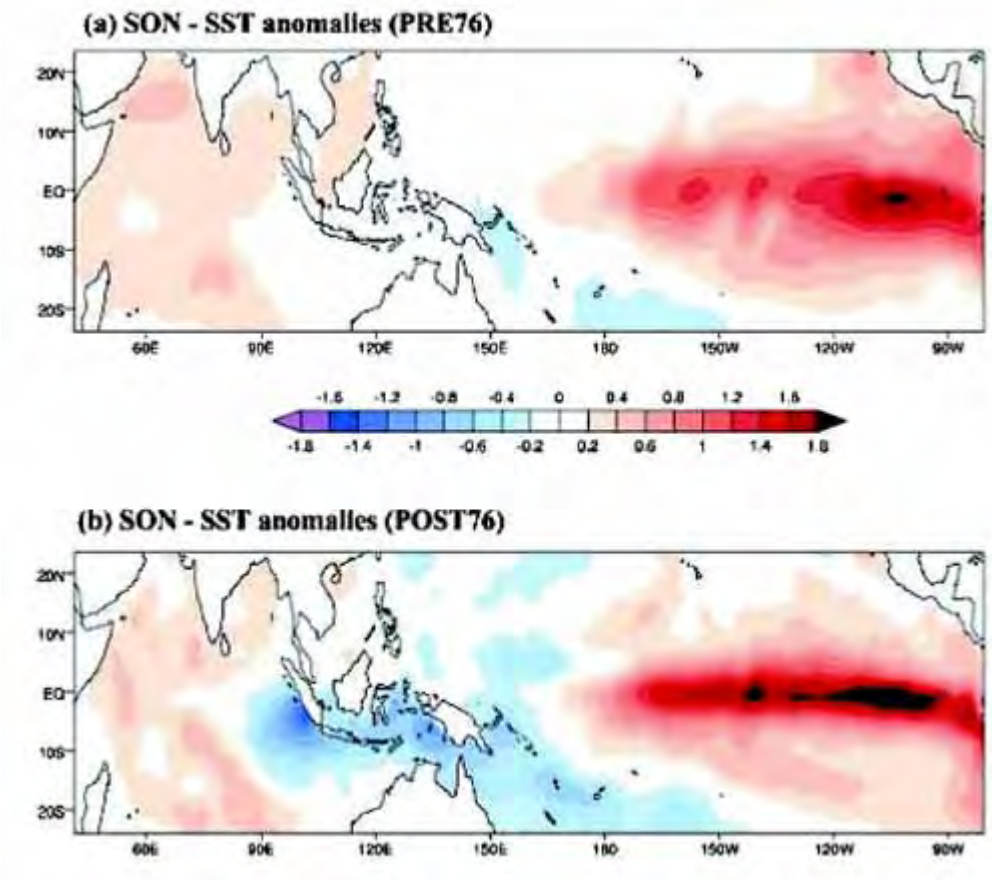

These IOBM events generate easterly wind anomalies over the western Pacific weakening El Nino growth. Co-occurrences with IOD, on the other hand, allow El Nino to grow.

Determining Indian Ocean impact on ENSO is difficult using statistical analysis as ENSO and Indian Ocean anomalies are intertwined. Some approached the problem by partial coupling techniques, but the results are contradicting (e.g., Wu and Kirtman 2004; Yu et al. 2009; Dommenget et al. 2006).

Figure source: Annamalai et al. 2005, J. Climate, 18.

CSIRO Mk3L

- Coupled GCM (atmosphere-ocean-land-ice) designed for millennial-scale climate simulations (*Phipps 2006, Technical Report No. 3, ACECRC, 236pp, ISBN 1-921197-02-X; see also Santoso et al. 2011, J Climate*)
- AGCM resolutions: 5.6^o lon x 3.2^o lat x 18 vertical
- OGCM resolutions: 2.8^o lon x 1.6^o lat x 21 vertical
- AGCM – CSIRO Mk3 (Gordon et al. 2002), OGCM – CSIRO Mk2 (Hirst et al. 2000), pre-industrial CO2 concentration (280ppm).
- **Experimental design**: run control (**CTRL**) setting for 400 years, continue to year 1500. For each 100-yr period from year 401, air-sea coupling is turned off in the Pacific and Indian Ocean basins, in turn (**dcpIO**, **dcpPO**), by forcing the AGCM within the coupled mode with the model's SST climatology.

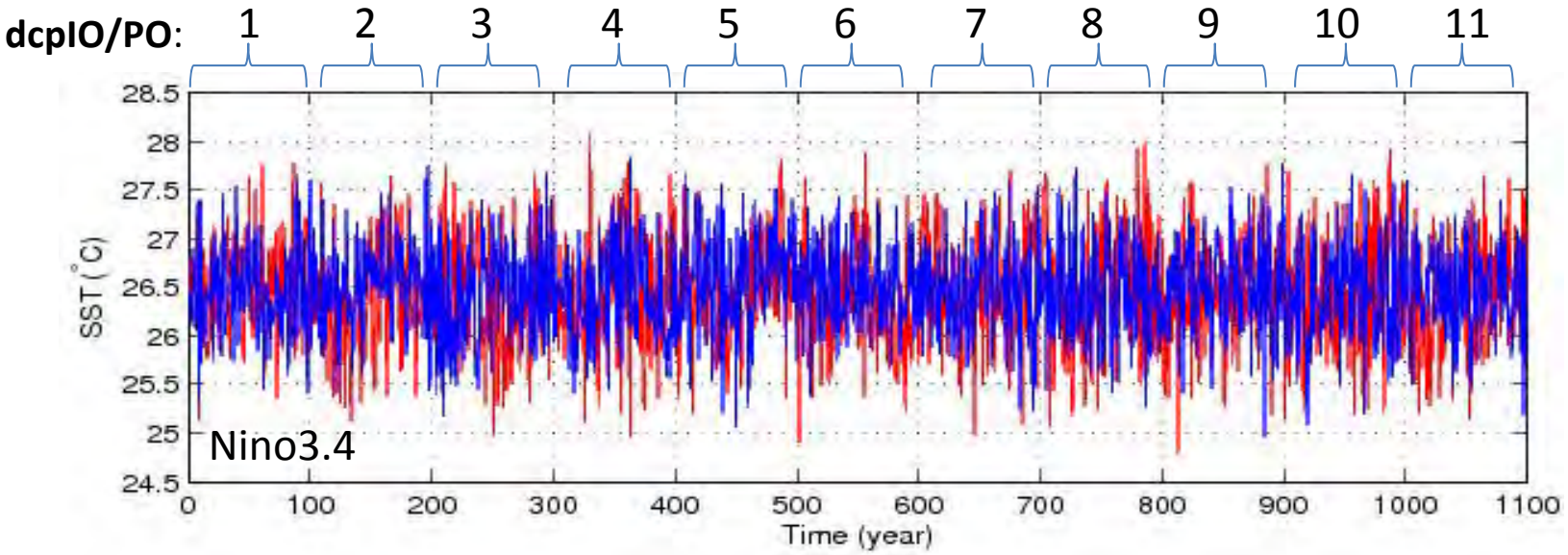

1st EOF maps showing El Nino, positive IOD, and warm IOBM SST anomalies

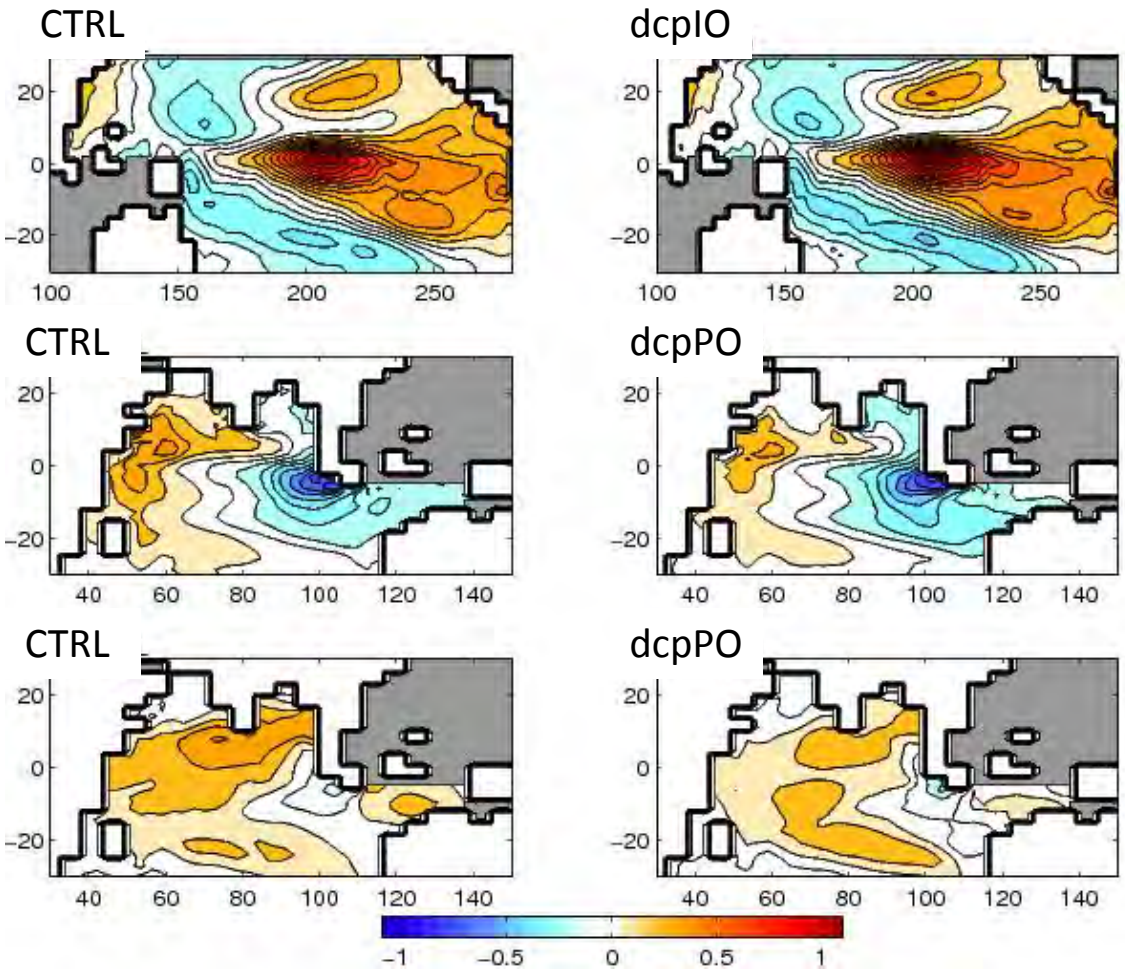

EOF1 (Sep-Dec)

EOF1 (Aug-Nov)

EOF1 (Jan-May)

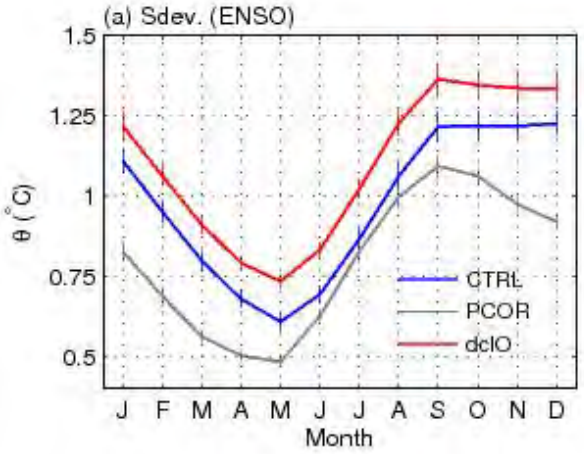

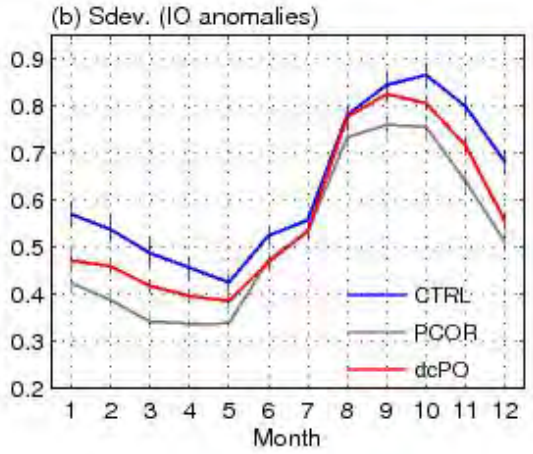

Partial correlation technique generally samples for weak ENSO.

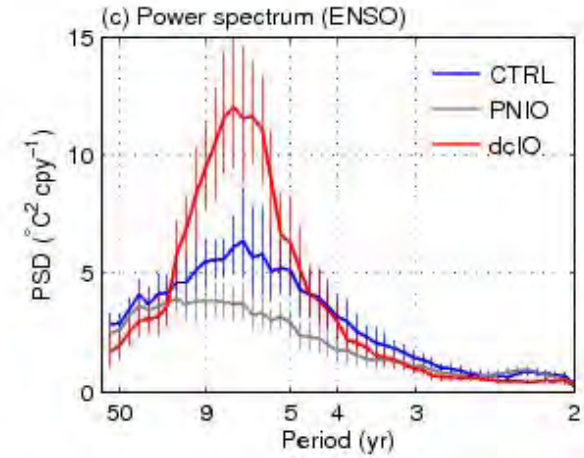

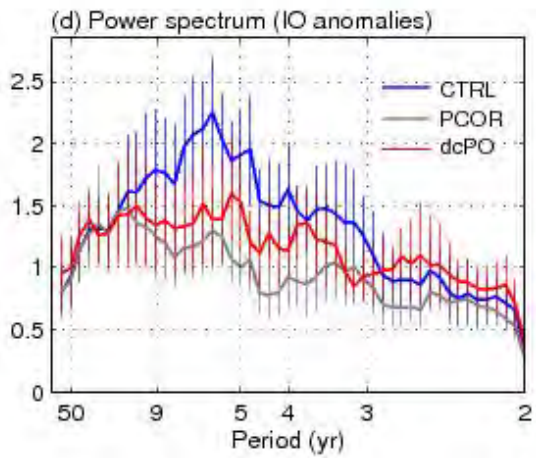

SON modes

The model simulates IOD and IOBM independent of ENSO, supporting the notion that IOD and even IOBM can occur without ENSO but with different characteristics (e.g., Behera et al. 2006, J Climate).

Note the spread of change in ENSO variability when the Indian Ocean is decoupled in each 100-yr period.

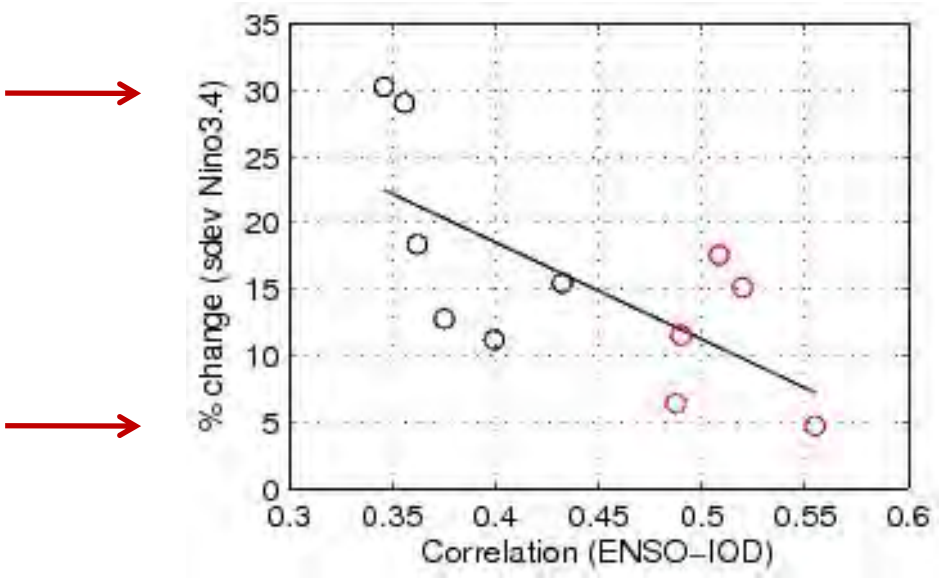

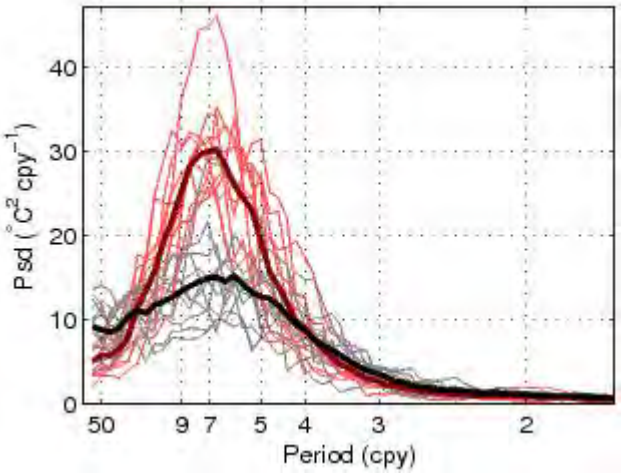

Can be as small as 5% increase but will unlikely ever be negative in this model.....
An indication the Indian Ocean plays a damping role on the simulated ENSO variability.

More prominent eastward propagating SST anomalies

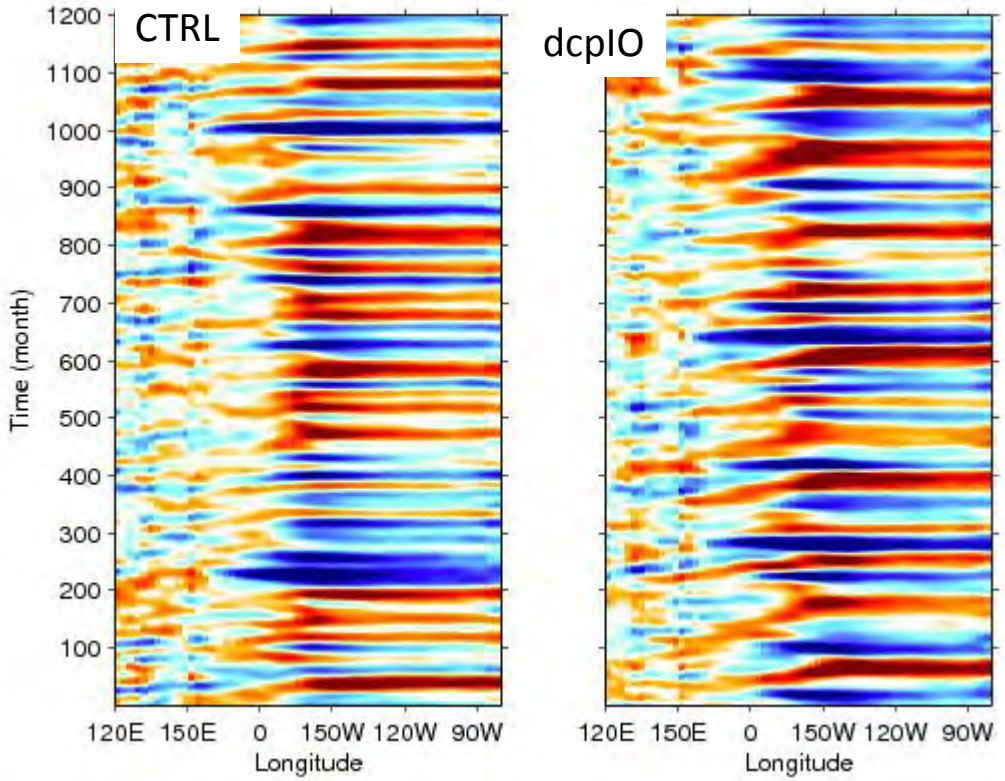

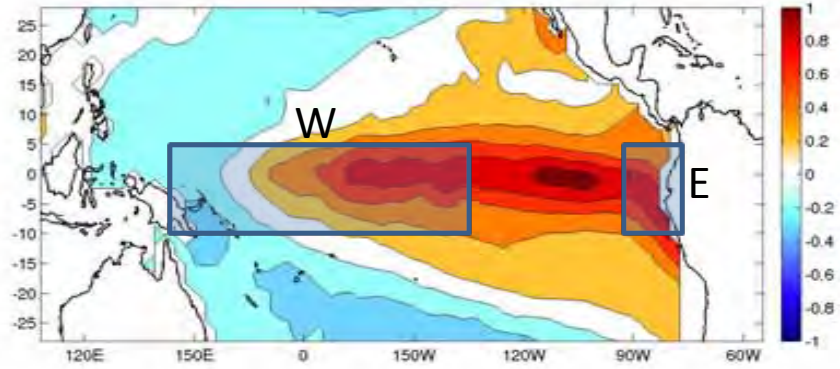

(See Guilyardi 2006, Climate Dyn., 26 , for a similar analysis)

Lag-correlation E-W vs Nino3

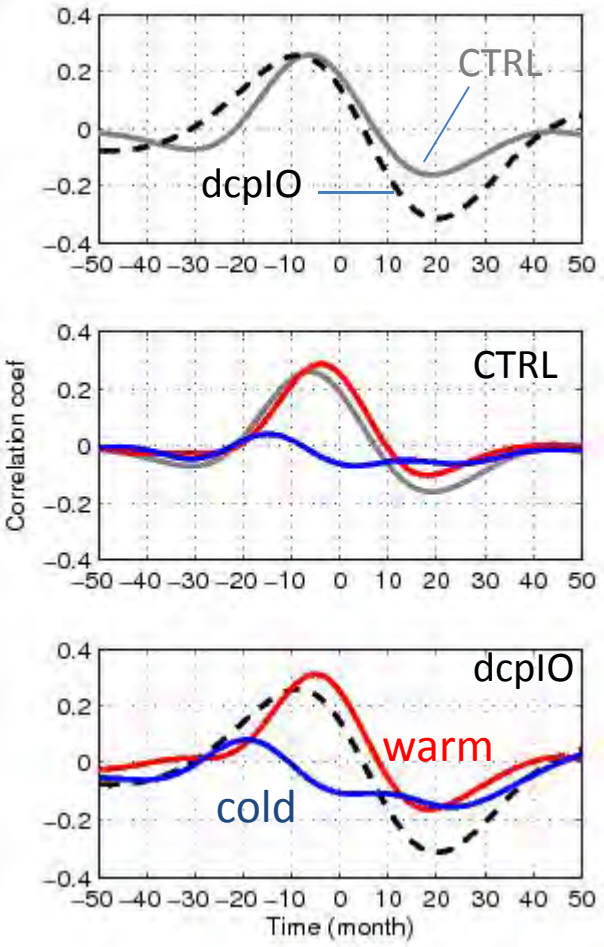

Nino3 leads Nino3 lags

Closed Indonesian Throughflow experiment (Santoso et al. 2011, *J Climate*)

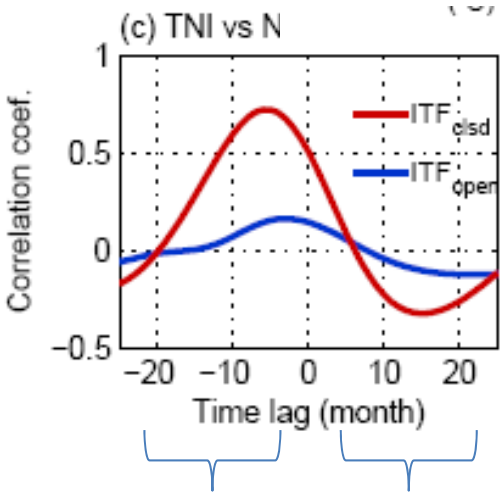

Nino3 leads TNI Nino3 lags TNI

TNI = Nino1.2 – Nino4

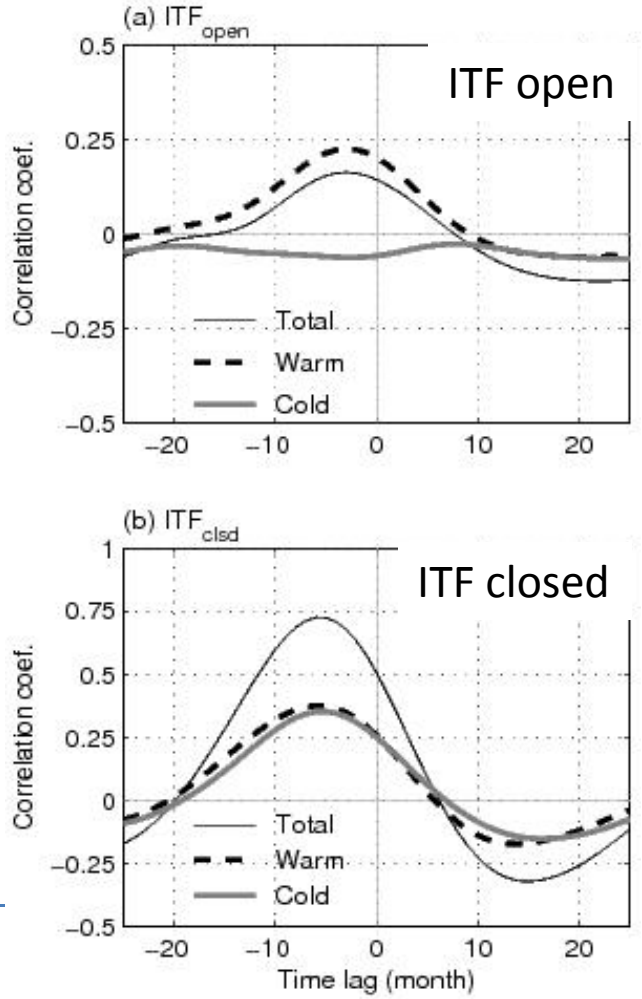

Now the symmetry in the propagation of warm and cold anomalies. The ENSO changes in the ITF closed experiment involve more complex processes than seen in the decoupling experiment.

BJ index formula (Jin et al. 2006, GRL; For applications see Kim and Jin 2011, *Clim Dyn*, Pt I and II; Santoso et al. 2011, *J Climate*)

$$2I_{BJ} \approx -\left(\frac{\langle \bar{u} \rangle}{L_x} + \frac{\langle -2y\bar{v} \rangle}{L_y^2} + \frac{\langle \bar{w} \rangle}{H_m}\right) - \alpha + \mu_a \beta_u \left\langle -\frac{\partial \bar{T}}{\partial x} \right\rangle + \mu_a \beta_w \left\langle \frac{\partial \bar{T}}{\partial z} \right\rangle + \mu_a^* \beta_h \left\langle \frac{\bar{w}}{H_m} \right\rangle$$

Mean currents (BJ_1) *Q damping (BJ_2)* *Zonal Adv (BJ_3)* *Ekman pumping (BJ_4)* *Thermocline (BJ_5)*

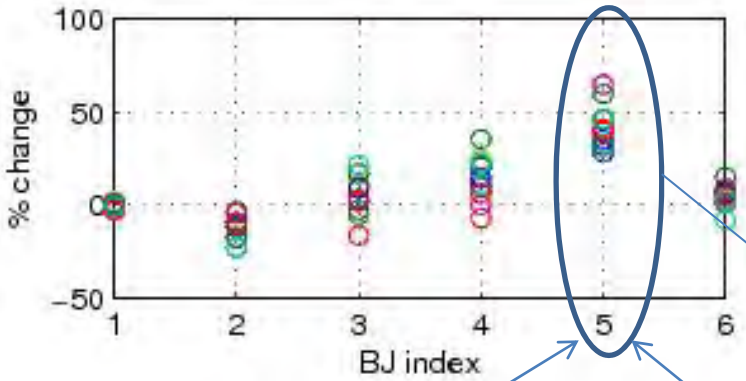

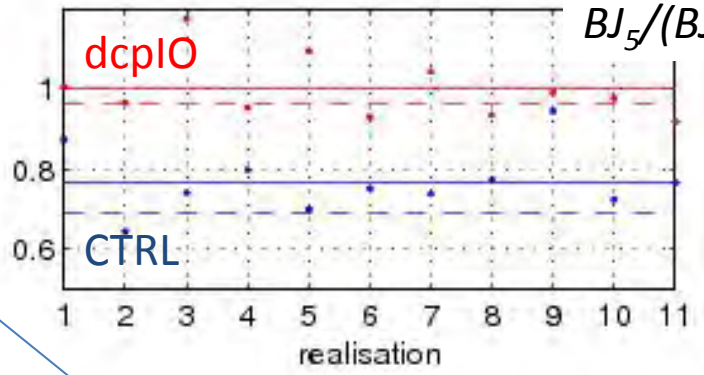

$BJ_5/(BJ_3+BJ_4)$

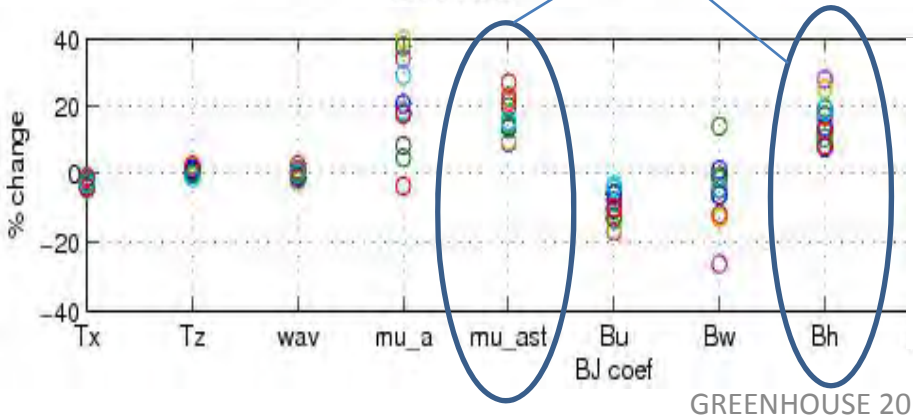

Enhanced thermocline feedback due to: 1) enhanced zonal wind – SST coupling, 2) zonal wind – east-west thermocline slope. Only subtle change in the mean climate.

$$[\tau^x] = \mu_a^* T_E$$

$$\mu_a^* = r([\tau^x], T_E)\frac{sd([\tau^x])}{sd(T_E)}$$

$$H_E - H_W = \beta_h[\tau^x]$$

$$\beta_h = r\left(H_E - H_W, [\tau^x]\right)\frac{sd\left(H_E - H_W\right)}{sd\left([\tau^x]\right)}$$

$\Delta r([\tau^x], T_E)$

$\Delta \dfrac{sd([\tau^x])}{sd(T_E)}$

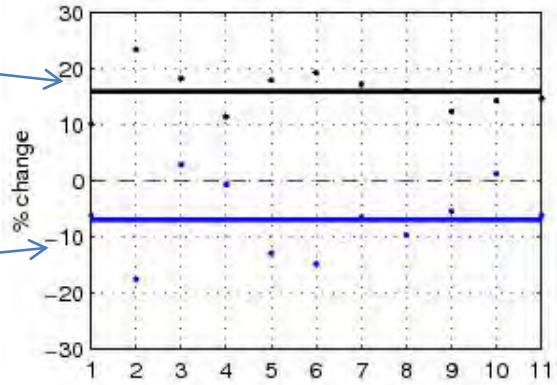

$r([\tau^x], T_E)$

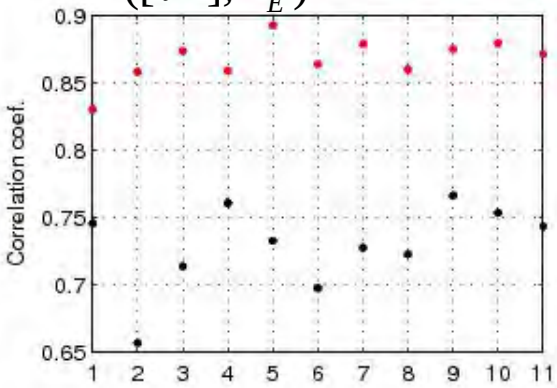

dcpIO

CTRL

$\Delta r\left(H_E - H_W, [\tau^x]\right)$

$\Delta \dfrac{sd\left(H_E - H_W\right)}{sd\left([\tau^x]\right)}$

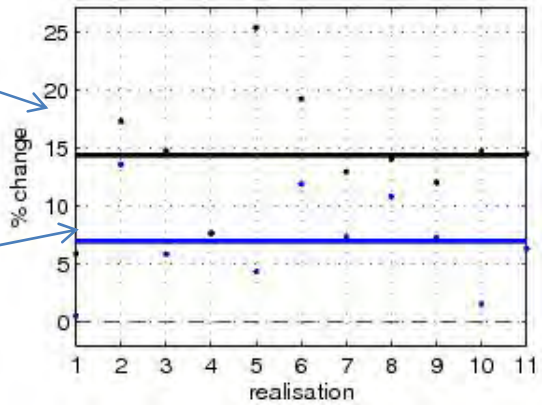

$r\left(H_E - H_W, [\tau^x]\right)$

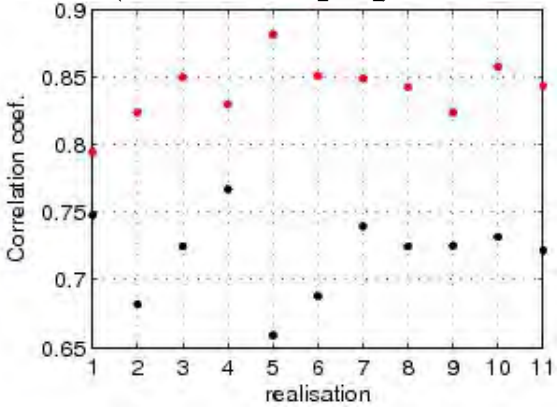

dcpIO

CTRL

Standard deviation of zonal wind stress over the equatorial Pacific

CTRL

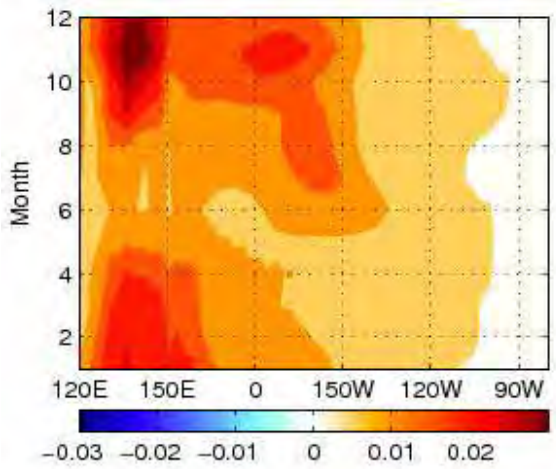

dcpIO-CTRL

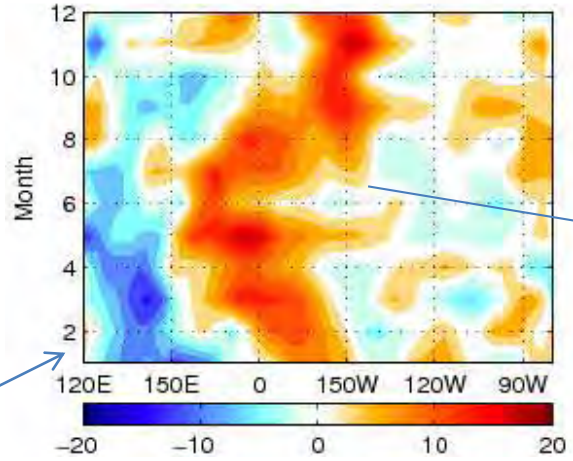

Stronger anomalies associated with stronger ENSO variability

Weaker anomalies in the western Pacific in dcpIO experiments.

El Nino composites

All realisations

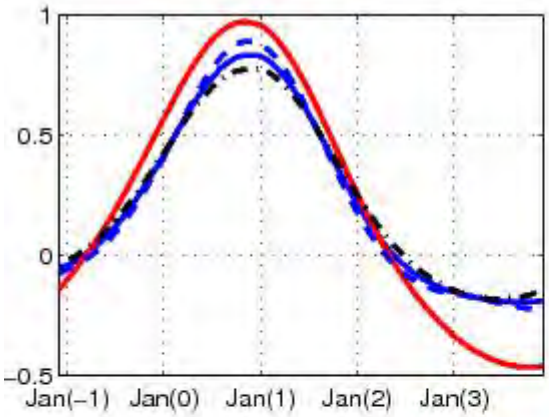

Strong ENSO-IOD correlation

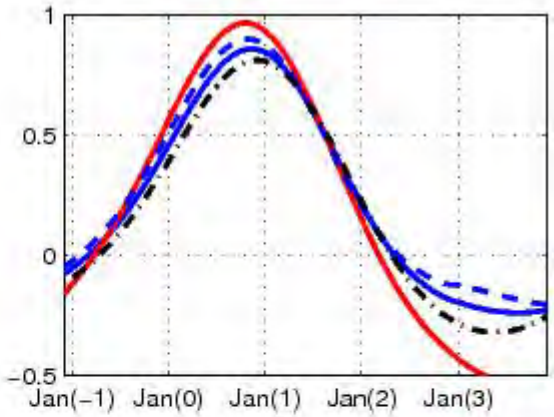

dcpIO

+ve IOD yr

Non +ve IOD yr

Weak ENSO-IOD correlation

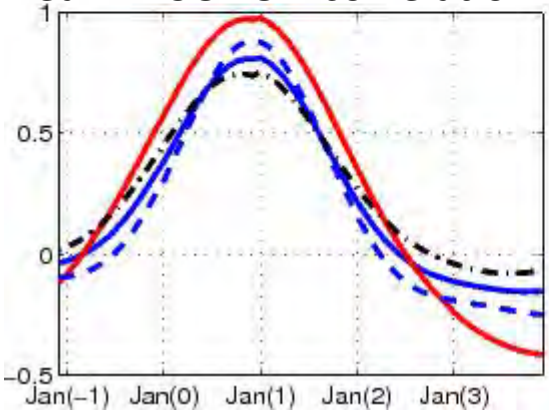

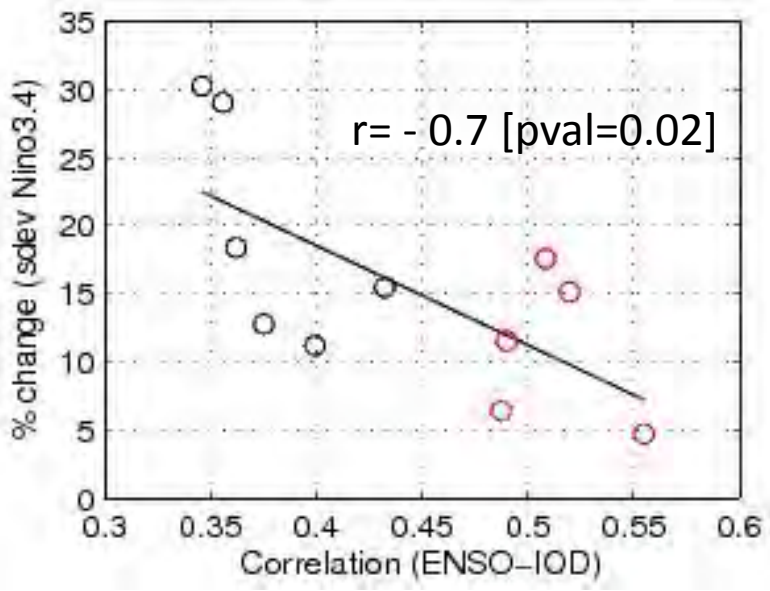

El Nino composites

+ve IOD yrs

Non +ve IOD yrs

All realisations

Strong ENSO-IOD correlation

Weak ENSO-IOD correlation

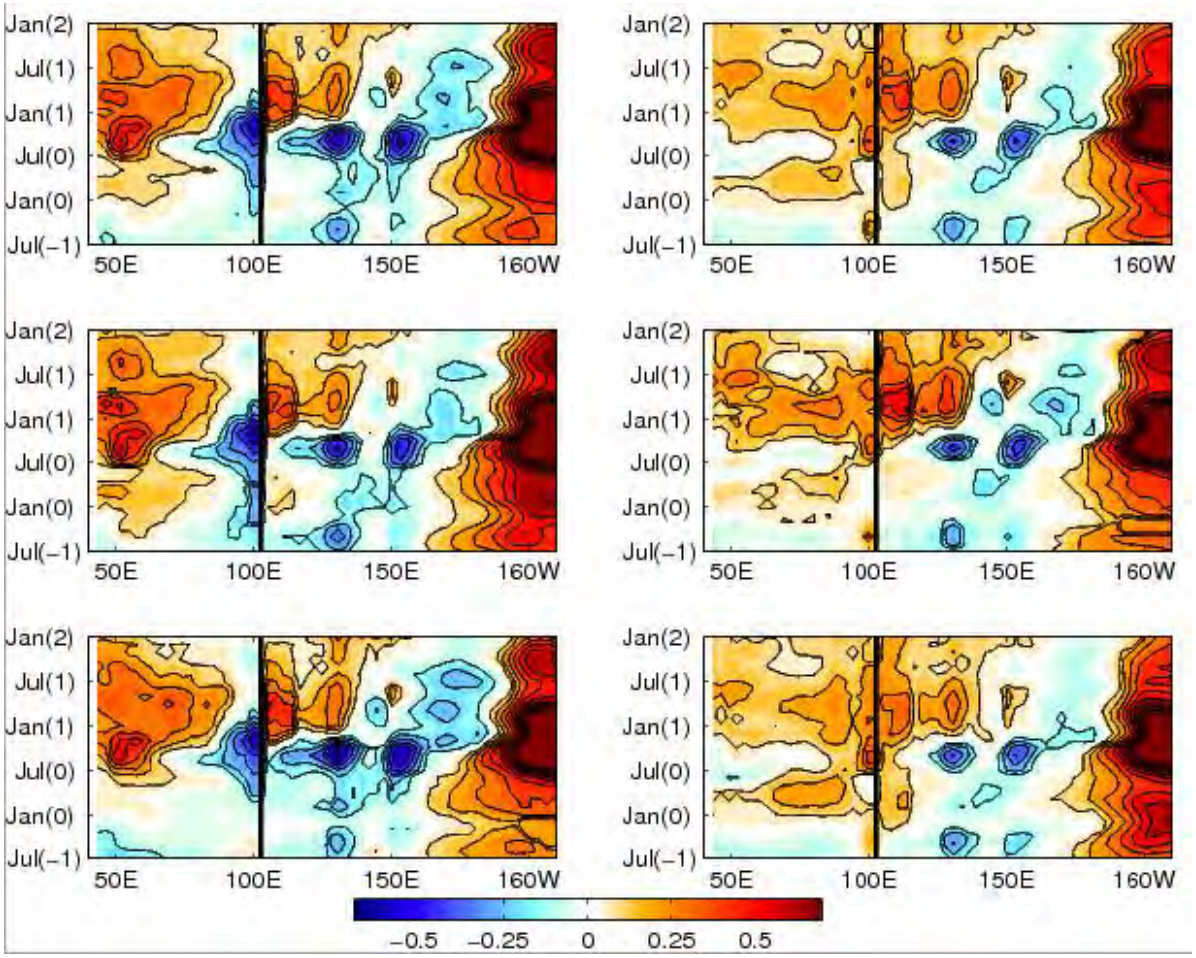

More prominent IOBM preceding ENSO

AGCM forced runs

A) El Nino SST in the Pacific

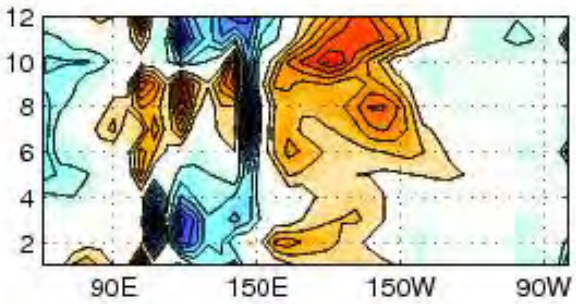

B) SST anomalies in Indian Ocean: IOBM (December-May) and IOD (June-November)

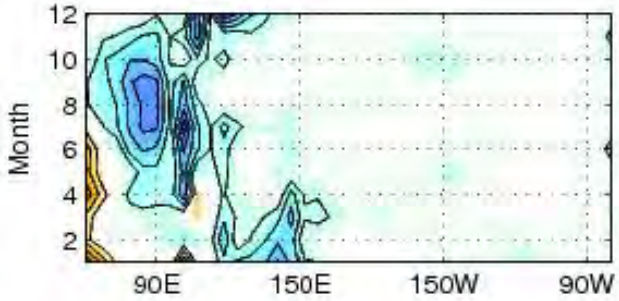

A) and B)

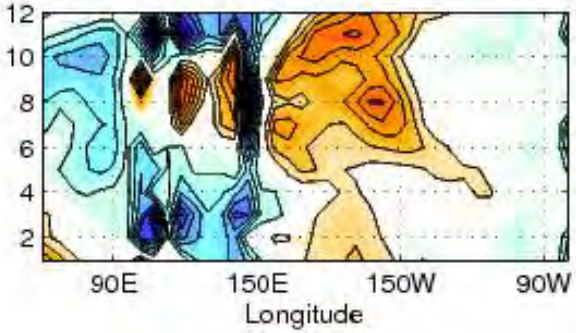

Boreal summer (JJA) rainfall anomaly composites

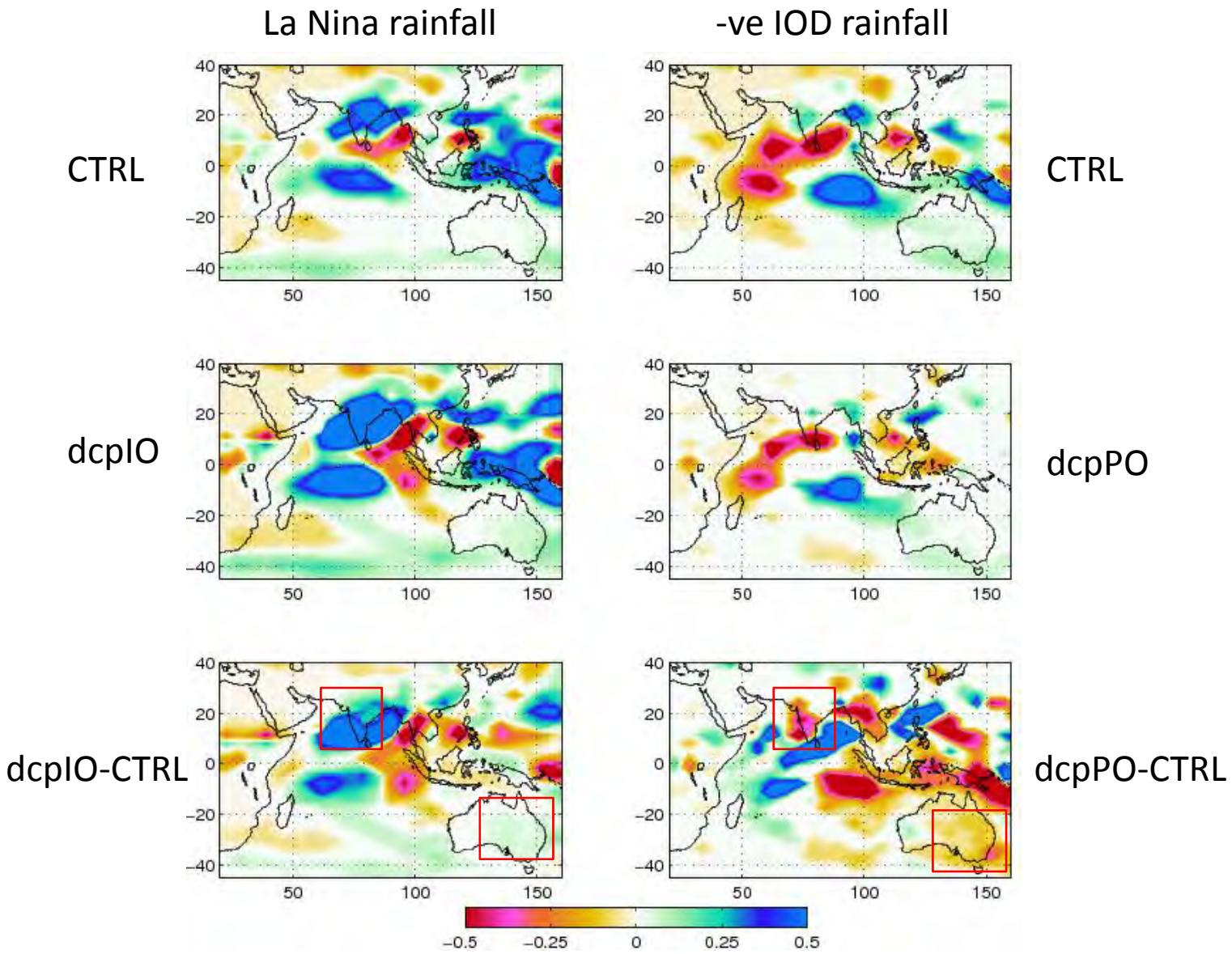

Boreal summer (JJA) rainfall composites

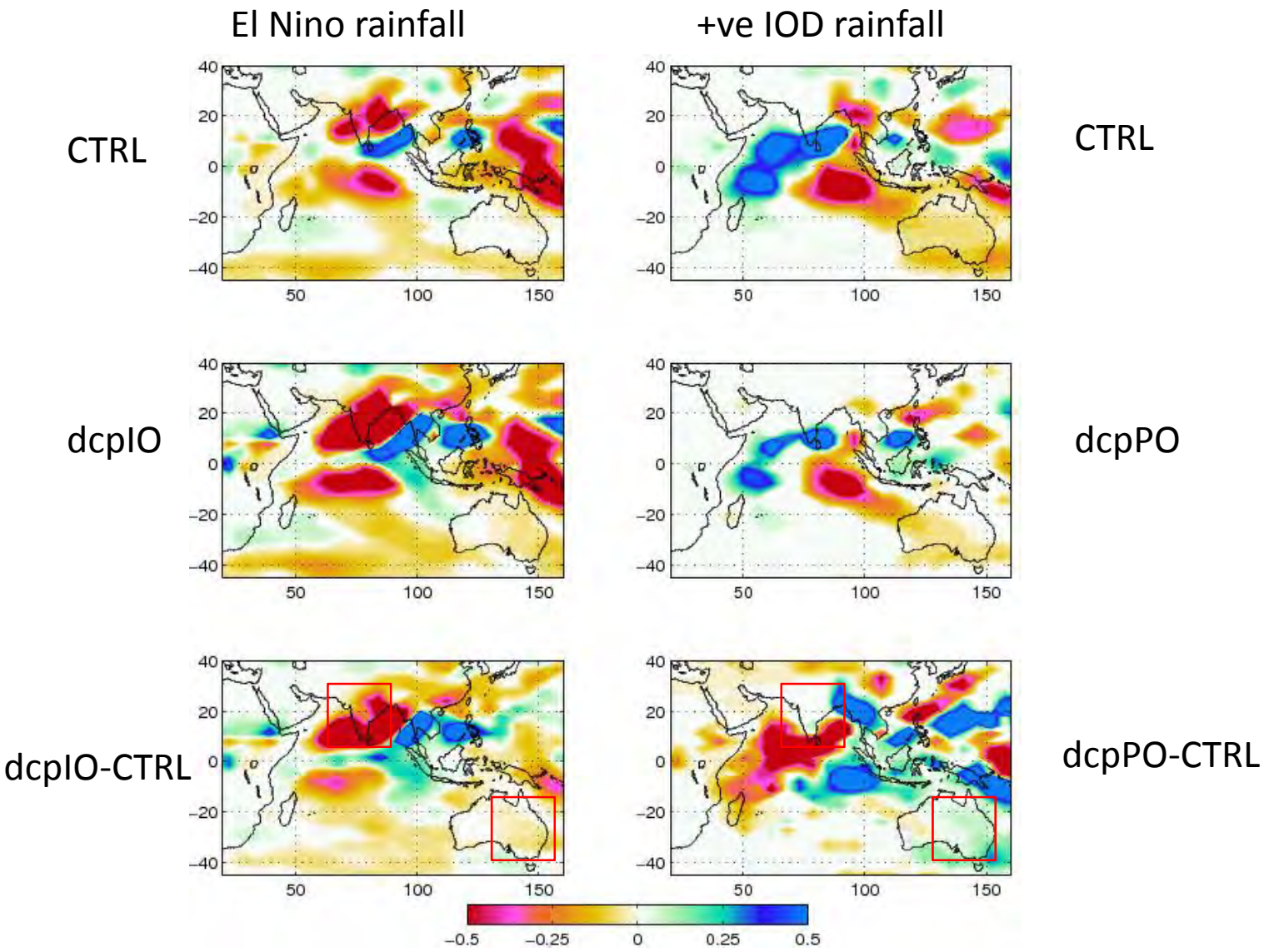

Boreal summer (JJA) SLP anomaly composites

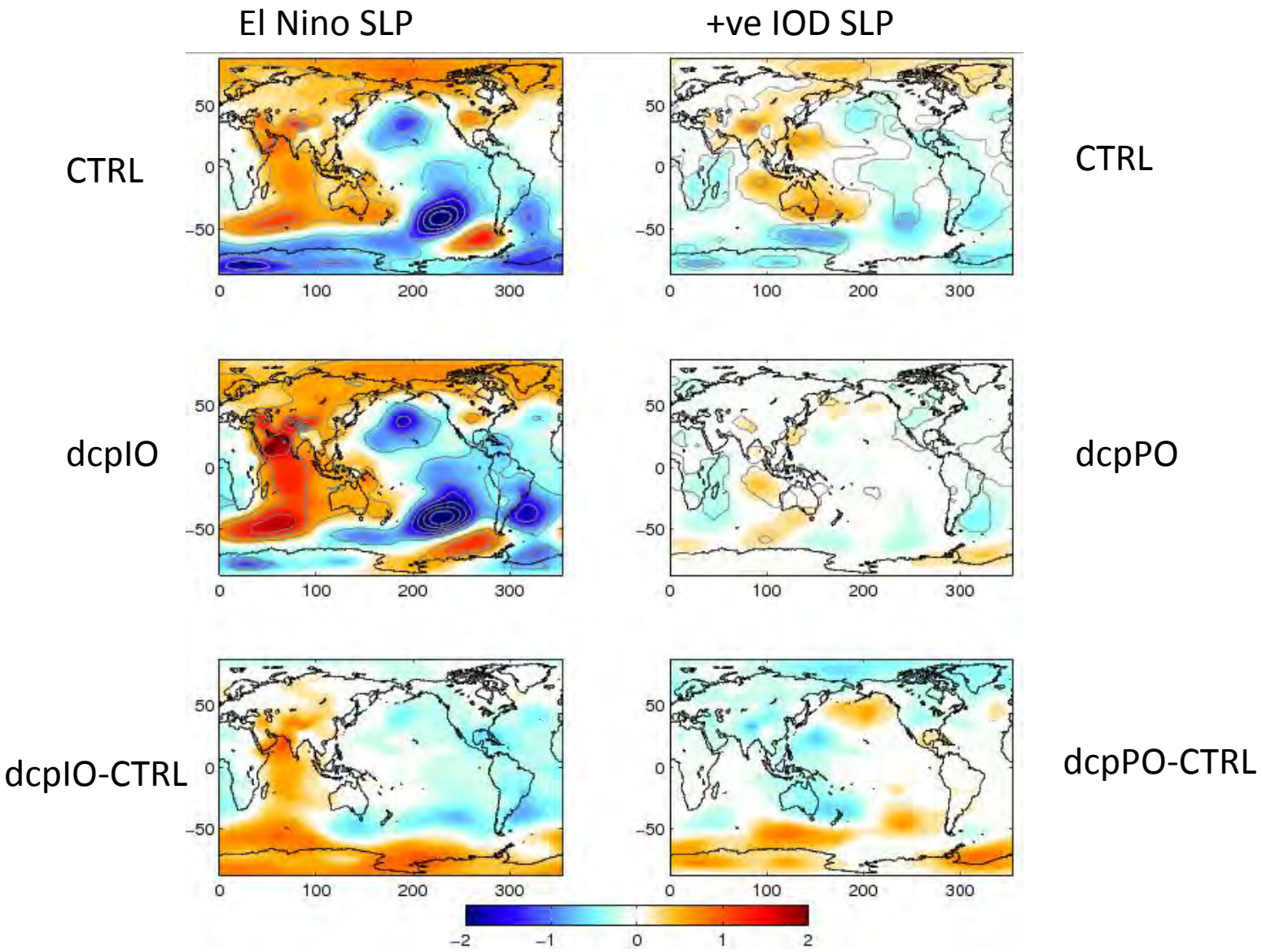

Summary

- It has been shown that Indo-Pacific interactions can influence ENSO behaviour. In CSIRO Mk3L, the ENSO thermocline mode becomes more prominent when the Indian Ocean is decoupled. This is due to stronger coupling between zonal wind stress and SST, and the east-west thermocline tilt. Weaker wind anomalies in the western Pacific influence this coupling. This appears to be due to the absence of the Indian Ocean Basin-wide Mode that often precedes ENSO in the control simulation, that otherwise has a damping effect on ENSO growth.
- It is likely that discrepancies among existing studies on the role of Indian Ocean on ENSO are not due to a limited sample size, but more to model biases (e.g., in terms of simulated ENSO regime and how it interacts with the Indian Ocean).
- The model's Indian Ocean overall acts to weaken ENSO variability. The ENSO on the other hand acts to energise the Indian Ocean anomalies. Such an interplay has implications on regional rainfall attribution and prediction.